Carbon – Science and Technology

ISSN 0974 – 0546

http://www.applied-science-innovations.com

ARTICLE Received :23/06/2010, Accepted :02/09/2010

Physicochemical properties of carbon materials obtained by combustion synthesis of perchlorinated hydrocarbons

S. Cudziło [(A)], M. Bystrzejewski [(B)], A. Huczko [(B)], M. Pakuła [(C)], S. Biniak [(D, *)], A. Świątkowski [(A)] and M. Szala [(A)]

(A) Military University of Technology, Kaliskiego 2, 00–908 Warsaw, Poland.
(B) Warsaw University, Pasteura 1, 02-093 Warsaw, Poland.
(C) Naval University of Gdynia, Smidowicza 69, 81-103 Gdynia, Poland.
(D) Nicolaus Copernicus University, Gagarina 7, 87-100 Toruń, Poland.

We present studies on the combustion synthesis of carbon materials from several perchlorinated organic compounds : tetrachloromethane (CCl_4), hexachloroethane (C_2Cl_6), tetrachloroethylene (C_2Cl_4), hexachloro-1,3-butadiene (C_4Cl_6), hexachlorocyclopentadiene (C_5Cl_6). The porosity (obtained by low-temperature nitrogen adsorption), microstructure (SEM), structural arrangement (XRD and Raman spectroscopy), surface chemistry (FTIR) and electrochemical behavior (cyclic voltammetry) of the obtained carbons were investigated. The synthesized materials exhibit an ordered structure similar to carbon black. Their physicochemical properties strongly depended on the structure of the perchlorocarbon precursor. It was found that perchlorinated compounds with unsaturated bonds yielded more amorphous products. The electrochemical properties (e.g. edl capacity) depend mainly on the mesopore surface area of the carbonaceous products.

1. Introduction : Combustion synthesis or self-propagating high-temperature synthesis [1] is a process that leads the formation of novel nanocarbons for fundamental studies as well as for potential applications. It has been recently found that such a synthesis is a simple and efficient route to produce nanomaterials like carbon nanoparticles [2], carbon encapsulates [3], exfoliated graphite [4] and silicon carbide nanowires [5]. Koch reported the detection of carbon nanotubes and carbon nano-carpet rolls in the reaction products of fluorinated graphite $(CF)_n$ with magnesium [6]. Multi-walled carbon nanotubes were found in the solid combustion products of a $CaC_2/C_2Cl_6/NaN_3$ mixture when ferrocene was used as a catalyst [7]. In an another study, we found that the thermolysis of NaN_3-C_6Cl_6 (or C_2Cl_6) system with the addition of ferrocene results in significant amounts of carbon-encapsulated iron nanoparticles [8].

In general, combustion synthesis (self-propagating high-temperature synthesis) with use of the chlorine-containing organic precursors leads to their destruction and the formation of non-hazardous carbonaceous materials with potential applications. Interest in the preparation of novel carbonaceous adsorbents has recently increased because of the theoretical nonpolar character of these materials for chromatography (e.g. HPLC), their applicability over a wide pH range, and the better defined surface properties in comparison to activated carbon [9]. The development of carbon sorbents suitable for analyte enrichment has generally paralleled the development of chromatographic sorbents. With the advent of gas chromatography attention turned to graphitized thermal carbon blacks and to novel active carbons prepared, for example, by the reduction of polytetrafluoroethylene with lithium amalgam [9].

Recently, we reported the use of hexachlorobenzene, hexachloroethane and their mixture as precursors in combustion synthesis initiated by sodium azide : the carbon materials thereby obtained possessed unique structural and surface properties, and the nature of the chlorine-containing substrate played an important role. In addition, the physicochemical properties of the carbons – porosity, crystallinity, adsorption capacity, electrochemical behavior, surface chemistry - varied according to the organic precursor used [10]. Materials obtained from perchlorinated aliphatic hydrocarbons turned out to be lower microporous, what can be

consistent with requirements for carbon sorbents to be applied in chromatography.

In the present work, tetrachloromethane, tetrachloroethylene, hexachloro-1,3-butadiene or hexachlorocyclopentadiene were used as oxidants, and the structural and surface properties of their reaction products with sodium azide (reducing agents) were examined. The aim of investigation is recognize of influence of precursor structure (alkenes, alkenes and cycloalkene) on physicochemical properties of obtained carbons. The relationship between the structure of the precursors and the structure of the carbonaceous products should make for a better understanding of the mechanism of the carbon structure formation. It is be possible in principle to produce carbon materials with a porosity range and surface properties tailored to specific requirements.

2. Experimental :

2.1 Conditions of synthesis : Powdered sodium azide (NaN_3) was mixed with tetrachloromethane (CCl_4), hexachloroethane (C_2Cl_6), tetrachloroethylene (C_2Cl_4), hexachloro-1,3-butadiene (C_4Cl_6) or hexachlorocyclo-pentadiene (C_5Cl_6) (the perchlorocarbons act as oxidants and carbon sources). Table (1) shows the composition of the tested mixtures corresponding to the equations of reactions assumed to yield free carbon, sodium chloride and nitrogen.The reaction mixtures (a paste when the organochlorine compound was in the liquid state) were formed into 10 g cylindrical samples and placed in a graphite crucible. The reaction was ignited electrically (ohmic heating).

Table (1) : Stoichiometry of the combusted mixture.

No	Assumed stoichiometry (wt% - organochlorine content)	Q (J/g)
1	CCl_4 (37.2) + $4NaN_3$ = C + 4NaCl + $6N_2$	1546
2	C_2Cl_4 (38.9) + $4NaN_3$ = 2C + 4NaCl + $6N_2$	2067
3	C_2Cl_6 (37.8) + $6NaN_3$ = 2C + 6NaCl + $9N_2$	2338
4	C_4Cl_6 (40.1) + $6NaN_3$ = 4C + 6NaCl + $9N_2$	2153
5	C_5Cl_6 (41.2) + $6NaN_3$ = 5C + 6NaCl + $9N_2$	2632

The combustion synthesis took place in an argon atmosphere (0.5 MPa) in a bomb calorimeter (to measure the heat of reaction - Q). The solid combustion products were flushed out of the reactor with water. To remove some of the side products like sodium chloride and sodium cyanide, the reaction products were heated under reflux in dilute hydrochloric acid and then rinsed with copious amounts of water. The suspension was filtered off, and the deposit rinsed with ethanol and dried.

2.2 Porosity and texture : The porosity of the combustion products was characterized by low-temperature nitrogen adsorption, the relevant isotherms [Figure (1)] of all samples were measured at 77.4 K on a Micromeritics ASAP 2010 volumetric adsorption analyzer (Norcross, GA, USA). Before each adsorption measurement, the sample was outgassed under vacuum at 200°C. The specific surface areas (S_{BET}) and mesopore areas (S_{me}) [11] as well as micropore volumes (V_{mi}) [12] were calculated from the adsorption isotherms. Scanning electron micrograph study was performed with a LEO 1430VP scanning electron microscope (SEM).

2.3 Spectroscopic analysis : X-ray diffraction (XRD) spectra were measured (D500 Diffractometer – Siemens) in conjunction with Cu Kα radiation, in the 2Θ range from 10° to 60° with a 0.05° step. Raman spectra (Jobin-Yvon T-64000) were collected from 1100 to 1800 cm^{-1} using a 514.5 nm excitation laser with a spectral resolution of 2 cm^{-1}. The spectra were deconvoluted and fitted using Lorentzian functions. Carbon-KBr mixtures (1.5 : 300) were ground, then desorbed at room temperature and pressed to obtain IR-transparent pellets, after which absorbance FTIR spectra of the carbon samples were recorded on a FTIR Spectrum 2000 Perkin-Elmer spectrometer.

2.2. Electrochemical studies : The cyclic voltammetry (CV) measurements were done with an Autolab (Eco Chemie) modular electrochemical system equipped with a PGSTAT 10 potentiostat driven by GPES3 software, together with the typical three-electrode electrochemical cell presented in one of our earlier papers [13]. A powdered carbon electrode (PCE), a Pt wire and a saturated calomel electrode (SCE) were used as the working, counter and reference electrodes, respectively. After vacuum desorption (10^{-2} Pa), the carbon sample (50 mg) was placed in an electrode container and drenched with a de-aerated solution to obtain a 3-5 mm sedimentation layer. The CV curves were recorded after establishment of electrochemical equilibrium (usually 20 hrs) [13] in blank solution (0.1 M monosodium phosphate in a water/ethanol mixture of volume ratio 3:1) without and with a depolarizer (0.05M $K_3[Fe(CN)_3$

3. Results and Discussion : Combustion synthesis yielded carbon materials with all the perchlorinated organic precursors (perchloroalkanes, perchloroalkenes and a cyclochloroalkene) used here. Table (2) lists their surface characteristics (mesopore surface area – S_{me} using DFT method [11]) and micropore volume – V_{mi} using Dubinin method [12]) estimated from low-temperature nitrogen adsorption isotherms.

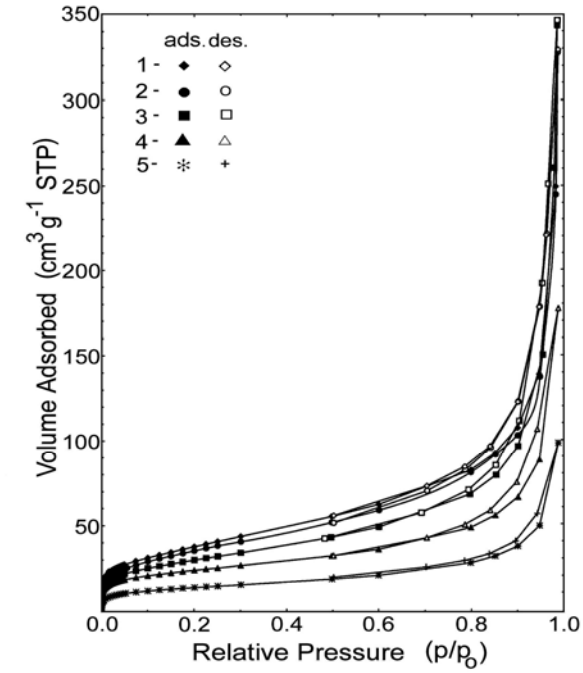

Figure (1) : Nitrogen adsorption-desorption isotherms at (77.4 K) of the combustion products: (1) C-C_5Cl_6, (2) C-CCl_4, (3) C-C_2Cl_6, (4) C-C_4Cl_6, (5) C-C_2Cl_4.

Table (2) : Surface characteristics of carbons.

No	Sample	S_{BET} m^2/g	S_{me} m^2/g	V_{mi} cm^3/g
1	C-CCl_4	130	32.0	0.075
2	C-C_2Cl_4	48	11.5	0.027
3	C-C_2Cl_6	99	19.9	0.058
4	C-C_4Cl_6	83	17.9	0.047
5	C-C_5Cl_6	137	26.2	0.081

The shapes of the nitrogen adsorption isotherms in the low and medium relative pressure range (for p/p_0 from about 0.1 to 0.7) are quite similar [Figure (1)]. In this range, the isotherms are nearly linear and have a relatively small slope.

When p/p_0 exceeds ~ 0.8, all the samples exhibit a dramatic increase in adsorption. The isotherms of the carbon materials resemble those of carbon black samples **[14]**. The amount of nitrogen adsorbed at the beginning of the hysteresis loop ($p/p_0 \approx 0.45$) is several times lower than the adsorption determined for maximal pressure achieved ($p/p_0 \approx 0.99$). Generally, obtained materials exhibit a microporosity near 5-10 times lower than typical activated carbon.

The SEM images of the carbon materials [Figure (2)] were differed depending on the kind of synthesis precursor. The images obtained for C_2Cl_4 to C_5Cl_6 [Figures (2b) - (2e)] were generally similar to those for carbon blacks **[15]**. The particles were spheroid in shape with a diameter near to or greater than 100 nm in the C- C_2Cl_4, and less than 100 nm in the C-C_5Cl_6 samples. The presence of a disordered phase or irregular particles was observed in the C-CCl_4 sample

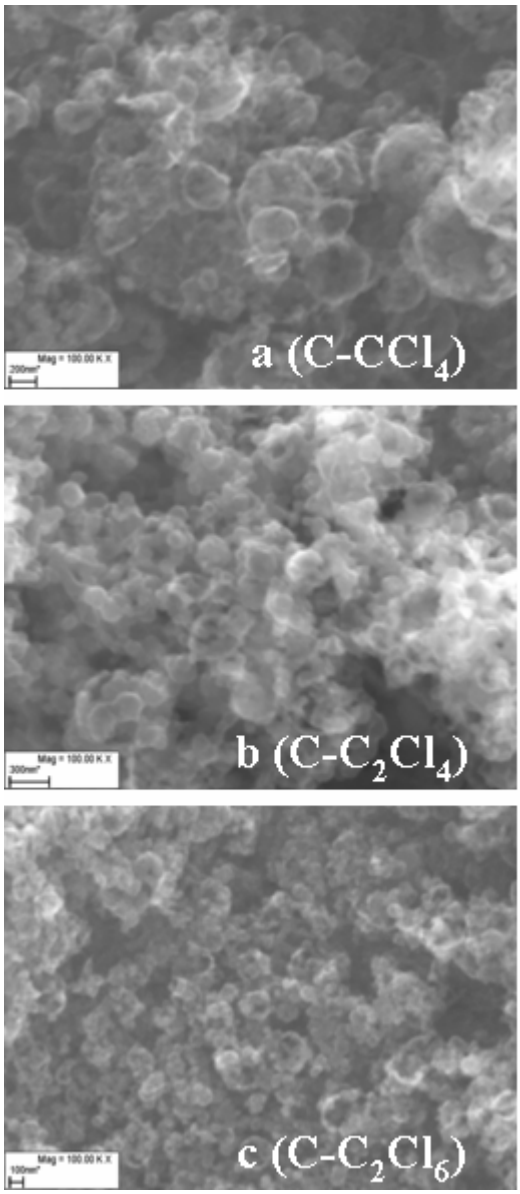

Figure (2) : SEM images of the combustion products : (a) C-CCl_4 (b) C-C_2Cl_4 c) C-C_2Cl_6 (d) C-C_4Cl_6 and (e) C-C_5Cl_6.

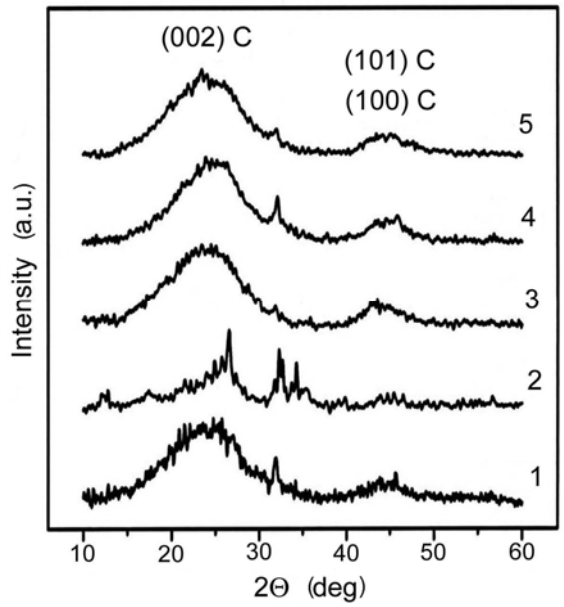

Figure (3) : X-ray diffraction spectra of the combustion products (numbers as in table 1).

Figure (3) shows the XRD diffraction patterns. The features located at 20-30º are ascribed to the (002) reflections of graphitic crystallites. The bands at 40-45º are less intense and correspond to the overlapping reflexes (100) and (101). The peak located at 31.7º is attributed to the (200) planes of NaCl crystallites. The pattern of the sample synthesized from C_2Cl_4 overlaps many diffraction lines, which may be due to the presence of disodium nitrosyl ($Na_2(NO)_2$). The bands corresponding to the carbon phase are considerably broadened as a result of the disordered structure **[16]**. The overlapping of the (100) and (101) carbon reflexes into one broad band also points to the lack of long-range periodicity along the graphene layers **[17]**. The (002) peak positions are between 23.4° and 24.4° (table 3), what corresponds to the average interlayer distance between 0.36 and 0.38 nm.

These values are higher than in single crystalline graphite (0.3354 nm), and they also exceed the values typical for turbostratic graphite (0.34-0.35 nm) **[18]**. A detailed analysis of the (002) profile can provide useful data concerning the structural disorder and the mean crystallite size, which is related with the full width at half maximum (FWHM) **[19]**. The obtained FWHM values lie in a narrow window and are between 9.5 and 10.8° (table 2). Such big FWHMs values are typical for amorphous carbons **[20]**. It also points that obtained carbon materials have similar crystallinity with very low stacking order in the adjacent graphene layers.

Table (3) : Structural parameters of carbons (from XRD and RS measurements)

No	XRD		Raman		
	2θ (200) (deg)	FWHM (002) (deg)	FWHM G (cm^{-1})	G/D	L_a nm
1	23.6	10.0	132	0.51	8.5
2	-	-	113	0.51	8.5
3	23.4	10.3	100	0.59	9.8
4	24.4	9.5	108	0.46	7.6
5	23.9	10.8	105	0.44	7.3

Further details regarding the structure of the products were obtained by Raman spectroscopy [Figure (4)]. The spectra were collected in the 1000-2000 cm^{-1} range, which corresponds to the wave number range providing the most valuable data on the structure of carbon materials. Two broad Raman bands appear at around 1300 and 1600 cm^{-1}. The latter band corresponds to the E_{2g} mode (stretching vibrations) in the basal graphene layer **[21]**.

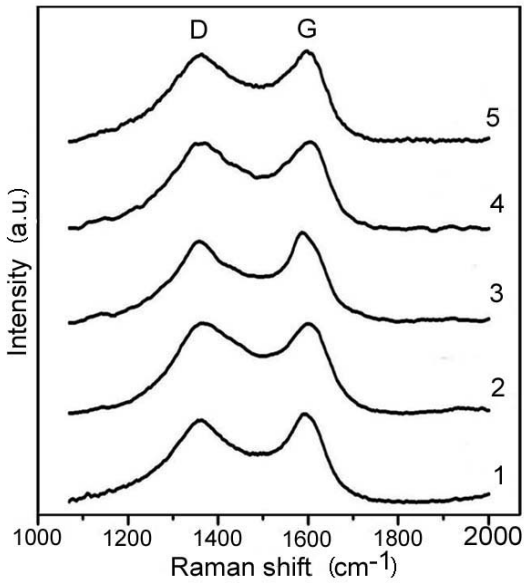

Figure (4) : Raman spectra of the combustion products (numbers as in table 2).

The width of this feature (FWHM G) is related to the extent of disorder within the plane aromatic layer, but it can be also used to obtain a rough estimate of the ordering between the stacked graphene layers (i.e. the width of the G band (table 3) corresponds to the d_{002} distance and L_c crystallite size) **[22]**. The D band located at 1300 cm^{-1} is associated with disorder; this forbidden mode becomes active owing to the lack of long-range order in amorphous and quasi-crystalline forms of carbon materials (symmetry breaking). The intensity of the D band can also be enhanced by the presence of small graphitic domains (finite size effect),

other imperfections such as substituted N or B atoms, sp^3 carbon, and the effects of finite particle size. The ratio between the integral intensities of G and D bands is a useful indicator of the degree of graphitization [23, 24]. In order to improve the accuracy of determinations of peak position, width or band integral intensity, curve deconvolution was performed (Lorentzian fitting). The position of the G band in all samples is upshifted by 10 -15 cm^{-1} compared to that in HOPG (1582 cm^{-1}). This is a consequence of the decrease in L_a (L_a is the diameter of the individual graphene basal plane) [19]. The G/D integral intensity ratio (Table 3) varies between 0.44 and 0.59. The carbon material synthesized from C_2Cl_6 has the highest G/D ratio and the lowest G bandwidth; this points to the greatest extent of crystallization and is consistent with X-ray diffraction results. L_a can be estimated from the following formula :

$$L_a = \frac{560}{E^4}\left(\frac{I_G}{I_D}\right) \qquad (1)$$

where E denotes the laser excitation energy, and I_G and I_D are the integral intensity of the G and D band, respectively [25].

The values of L_a are between 7.6 nm and 9.8 nm and are 20-30% higher than those obtained for amorphous carbons times higher similar to those for amorphous carbons [20]. Interestingly, the higher graphitization in the *a* direction was found for samples 1-3, i.e. where the chlorine content in the starting combusted mixture was the lowest. Presumably, the chlorine may influence the formation of graphene layers during the course of the reaction leading to the low ordered structures. The mechanism of this phenomenon can be similar to that one reported for fullerene synthesis [26]. It was shown, that chlorine dramatically reduced the fullerene yield. Chlorine saturated the freshly formed large carbon cluster and hampered their aggregation in fullerene molecules. We believe that similar scenario took place in our reaction system.

The FTIR spectra [Figure (5)] exhibit bands characteristic of (i) the –OH moiety (structural hydroxyl functional groups and adsorbed water molecules), (ii) the overlapping bands of aromatic C=C skeletal vibration and C=O structural stretching vibrations (isolated or conjugated quinones, ion-radical structures and conjugated systems like diketone and keto-enol) and (iii) the C-O-C groups (oxygen bridges) with respective maxima at 3450, 1600 and 1220 cm^{-1} [27 - 29]. Since H_2O is sorbed on the surface of carbon materials with the participation of interactions both specifics (hydrogen bonds, chemisorption due to surface oxide hydration) and non-specific (physical adsorption), the bands in the 1600-1500 cm^{-1} region can also be partially described by OH bonding vibrations. The partially resolved peaks forming the absorption band in the 1260-1000 cm^{-1} region can be assigned to C-O symmetrical stretching vibrations in ether- (>C-O-C<), ester- (-O=C-O-C<) and phenolic-like (>C-OH) structures existing in different structural environments.

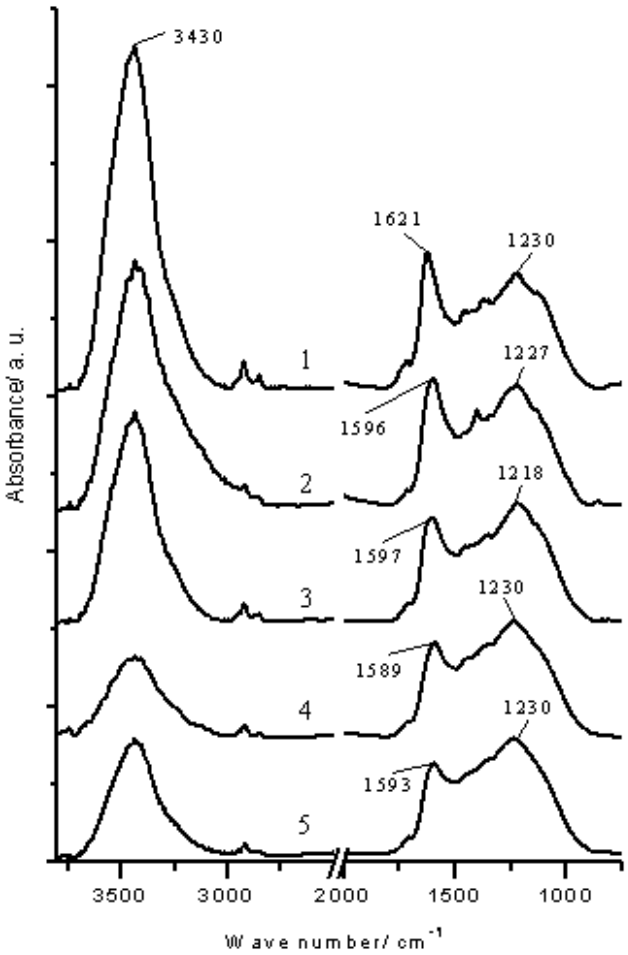

Figure (5) : FTIR transmittance spectra of the carbon materials (KBr pellets) (numbers as in Table 1).

The KBr-pellet technique applied here precludes a quantitative comparison of the FTIR spectra obtained for the different carbons, but if does indicate which individual chemical structures may or may not be present in the carbon. The changes in the relative intensity of the bands in the samples tested [Figure (5)] can be interpreted as the resulting from various surface reactions of the freshly obtained carbon surface with oxygen and water molecules during preparation (removal of inorganic salts). The increase in the relative intensity bands due to –OH and C=O moieties (samples 1-3) indicates a higher degree of surface oxidation. Some of these surface groups can exhibit electrochemical activity [28]. The relative greater intensity of the bands near 1230 cm^{-1} (sample

3-5) indicates the presence of mainly structural C-O-C moieties in the carbon network. The intensity of the FTIR absorption bands due to oxygen species in C-C_4Cl_6 and C- C_5Cl_6 samples is relatively smaller [Figure (5)]. Interestingly, the products obtained from precursors with double C=C bonds have a weaker affinity for oxygen. The electrochemical behavior of powdered carbon electrodes prepared from the test materials depended to a large extent on their surface chemistry and texture [Figures (6) and (7)].

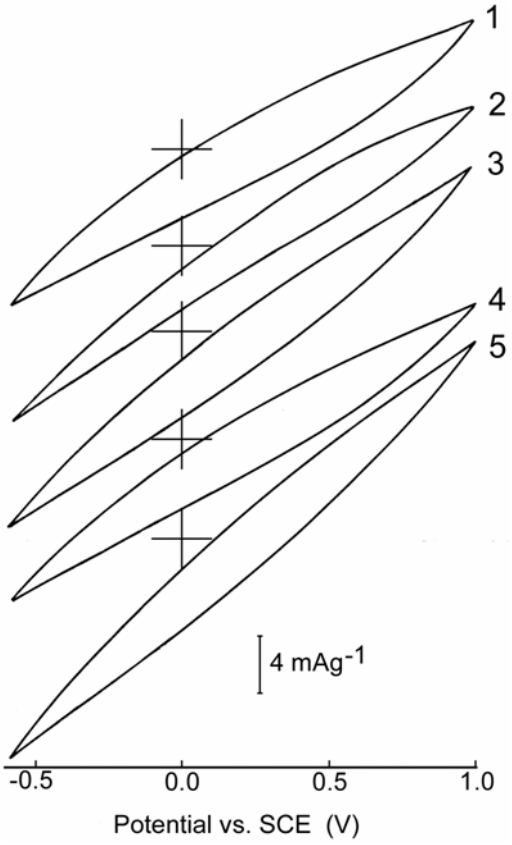

Figure (6) : Cyclic voltammograms of the carbon electrode materials (numbers as in table 1) recorded in a mixed electrolyte (75 ml aq. 0.1 M NaH_2PO_3 and 25 ml ethanol) solution; sweep rate v = 1 mV/s.

CV experiments of electrodes were performed in the potential window between –0.6 V to + 1.0 V vs. SCE in weak acidic buffer solution. The capacitive currents were visible only on the CV curves for all samples in blank solutions [Figure (6)]. The electric double layer capacities (C_{dl}) for zero potential values were read off the curves **[30]** :

$$C_{dl} = i/v \qquad (2)$$

where i is the capacitive current (mA/g) and v is the sweep rate (mV/s).

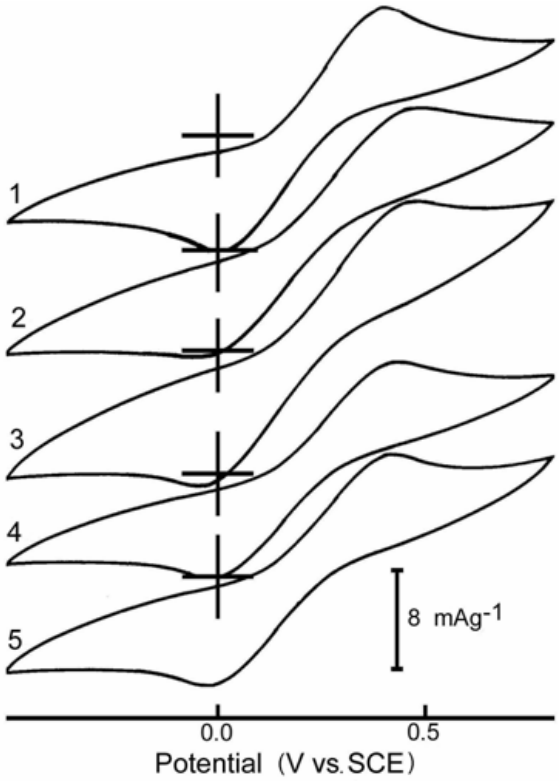

Figure (7) : Cyclic voltammograms of the $[Fe(CN)_6]^{4-}$/ $[Fe(CN)_6]^{3-}$ couple on carbon electrodes (numbers as in table 1); v = 2 mV/s.

CV curves were also recorded in the presence of a ($Fe(CN)_6^{4-}$/ $Fe(CN)_6^{3-}$) couple as depolarizer [Figure (7)], exhibiting quasi-reversible anodic and cathodic peaks.

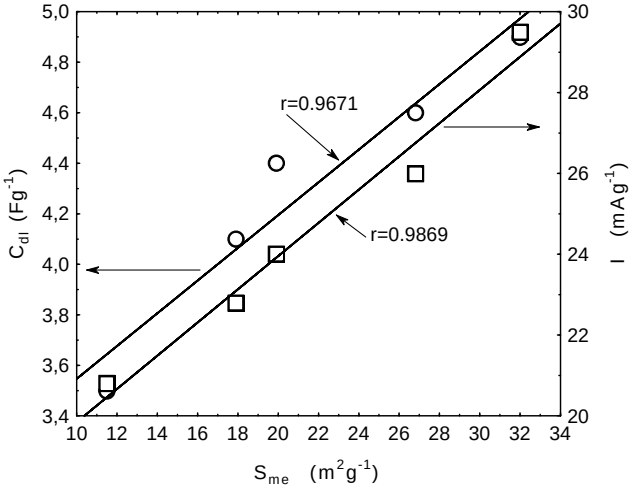

Figure (8) : Dependences of electrochemical capacity (C_{dl}) and anodic peak current ($I_{p,a}$) on the mesopore surface area of carbon electrode materials.

The relation between peak intensity of anodic current and ($I_{p,a}$) and the square of the sweep rate is linear (regression coefficient near 0.99) over the rate range used (1-7.5 mV/s). Both C_{dl} and $I_{p,a}$ also exhibited a

mesopore surface area with good linear correlation [Figure (8)]. However, it was demonstrated that not only the surface area, but also the electronic **[31]** and structural properties **[32, 33]** of porous carbon materials, and their surface chemistry **[34, 35]** can affect their electric double layer capacitance. The linear relationship between the electric double layer capacity and mesopore surface area indicate that these features play the main role in ion loading during electrode polarization.

4. Conclusion : Carbonaceous materials obtained from the combustion of perchlorinated organics exhibit similarities to carbon blacks. A number of correlations were found between the parameters characterizing the internal structure, surface texture, surface chemistry and electrochemical behavior in a series of tested samples :

(a) aliphatic precursors yield carbon materials of a higher crystallinity, whereas perchlorocarbons with unsaturated C=C bonds yield more amorphous materials with smaller lamellae;

(b) the surface area of the carbons obtained seems to be independent of the kind of precursor; however, the products from precursors with double C=C bonds are more resistant to surface oxidation;

(c) both the electrical double layer capacity of powdered electrodes and the investigated electron-change reaction depend mainly on the mesopore surface area of the electrode carbon materials.

References :

[1] A. Varma, S. Rogachev, A. Mukasyan, S. Hwang, Adv. Chem. Eng. 24 (1998) 79.

[2] S. Cudziło, M. Bystrzejewski, H. Lange, A. Huczko, Carbon 43/8 (2005) 1778.

[3] M. Bystrzejewski, A. Huczko, H. Lange, P. Baranowski, W. Kaszuwara, S. Cudziło, E. Kowalska, M. Rummeli, T. Gemming, Fullerenes Nanotubes and Carbon Nanostructures 16/4 (2008) 217.

[4] S. Cudziło, M. Szala, A. Huczko, M. Bystrzejewski, Prop. Explos. Pyrotech. 32/2 (2007) 149.

[5] A. Huczko, M Bystrzejewski, H. Lange, A. Fabianowska, S .Cudziło, A. Panas, M. Szala, J. Phys. Chem. B 109 (2005) 16244.

[6] E.-C. Koch, Prop. Explos. Pyrotech. 30/3 (2005) 209.

[7] M. Szala, Int J. S.H.S. 17 (2008) 106.

[8] M. Bystrzejewski, A. Huczko, H. Lange, S. Cudziło, W. Kiciński, Diam. Relat. Mater. 16 (2007) 225.

[9] B. Buszewski, M. Michel, Porous graphitized carbon as stationary chase for separation technologies. In: A.P. Terzyk, P.A. Gauden, P. Kowalczyk (Eds), Carbon Materials: Theory and Practice, Research Signpost, Trivandrum, 2008, p. 209.

[10] S. Cudziło, A. Huczko, M. Pakuła, S. Biniak, A. Świątkowski, M. Szala, Carbon 45/1 (2007) 103.

[11] C. Lastoskie, K.E. Gubbins, and N. Quirke, J. Phys. Chem. 97 (1993) 4786.

[12] S.J. Gregg, K.S.W. Sing, Adsorption, surface area and porosity, Academic Press; London, 1982.

[13] S. Biniak, A. Świątkowski, M. Pakuła, Electrochemical studies of phenomena at active carbon-electrolyte solution interfaces. In : L.R. Radovic, editor. Chemistry and Physics of Carbon, vol. 27. Marcel Dekker Inc, New York – Basel, 2001, p. 125.

[14] M. Kruk, M. Jaroniec, Y. Bereznitski; J. Colloid Interface Sci. 182 (1996) 282

[15] J.-B. Donnet, R.C. Bansal, M.-J. Wang, Carbon black. Science and technology, Marcel Dekker, New York, 1993, p. 104.

[16] J. A. Nisha, J. Janaki, V. Sridharan, G. Padma, M. Premila, T.S. Radhakrishnan, Thermochim Acta 286/1 (1996) 17.

[17] M. Käärik, M. Arulepp, M. Karelson, J.Leis, Carbon 46/12 (2008) 1579.

[18] Z.Q. Li, C.J. Lu, Z.P. Xia, Y. Zhou, Z. Luo, Carbon 45/8 (2007) 1686.

[19] N. Iwashita, C.R. Park, H. Fujimoto, M. Shiraishi, M. Inagaki, Carbon 42/4 (2004) 701.

[20] L. Lu, V. Sahajwalla, C. Kong, D. Harris, Carbon 39/12 (2001) 1821.

[21] F. Tuinistra, J.L. Koenig, J. Chem. Phys. 53 (1970) 1126.

[22] A. Yoshida, Y. Kaburagi, Y. Hishiyama, Carbon 44/11 (2006) 2333.

[23] Y. Wang, D.C. Alsmeyer, R.L. McCreery, Chem. Mater. 2 (1990) 557.

[24] A.C. Ferrari, S.E. Rodil, J. Robertson, Phys. Rev. B 67 (2003) 155306.

[25] M.R. Baldan, E.C. Almeida, A.F. Azevedo, E.S. Golcaves, M.C. Rezende, N.G. Ferreira, Appl. Surf. Sci. 254/2 (2007) 600.

[26] H. Richter, E. de Hoffmann, E. Doome, A. Fonseca, J.-M. Gilles, J.B. Nagy, et al., Carbon 34/6 (1996) 797.

[27] P.E. Fanning, M.A. Vannice, Carbon 31/5 (1993) 721.

[28] S. Biniak, M. Pakuła, A. Świątkowski, M. Walczyk, in : A. P. Terzyk, P. A. Gauden, P. Kowalczyk (Eds), Carbon Materials : Theory and Practice, Research Signpost, Trivandrum : 2008, p. 51.

[30] K. Kinoshita, Carbon : Electrochemical and Physicochemical Properties. New York: John Wiley & Sons. (1988).

[31] B. Kastening, M. Hahn, B. Rabanus, M. Heins,

U. Felde, Electrochim. Acta 42 (1997) 2789.
[32] C. Portet, G. Yushin, Y. Gogotsi, Carbon 45 (2007) 2511.
[33] C. Portet, J. Chmiola, Y. Gogotsi, S. Park, K. Lian, Electrochim. Acta 53 (2008) 7675.
[34] M. J. Bleda-Martinez, J. A. Macia-Agullo, D. Lozano-Castello, E. Morallon, D. Cazorla-Amoros, A. Linares-Solano, Carbon 43 (2005) 2677.
[35] C. T. Hsieh, H. Teng, Carbon 40 (2002) 667.

Advertisement :